Desalination and Water Treatment
www.deswater.com
doi: 10.1080/19443994.2015.1041054

57 (2016) 9609–9621
May

Taylor & Francis
Taylor & Francis Group

Nanofiltration treatment of tomato paste processing wastewater: process modeling and optimization using response surface methodology

Ali Alghooneh[a], Seyed M.A. Razavi[a,*], Seyed Mahmoud Mousavi[b]

[a]*Division of Food Engineering, Department of Food Science and Technology, Ferdowsi University of Mashhad (FUM), P.O. Box: 91775-1163, Mashhad, Iran, Tel. +98 511 8795620; Fax: +98 511 8763842; emails: Alghooneh.Ali@um.ac.Ir (A. Alghooneh), S.Razavi@um.ac.Ir (S.M.A. Razavi)*
[b]*Department of Chemical Engineering, Ferdowsi University of Mashhad (FUM), P.O. Box: 91775-1111, Mashhad, Iran, Tel. +98 511 8816840; Fax: +98 511 8816840; email: mmousavi@um.ac.ir*

Received 11 September 2014; Accepted 19 March 2015

ABSTRACT

Tomato wastewater is characterized by a large amount of suspended solids, red color, and bad smell. In this paper, the effect of transmembrane pressure (10, 15, 20 bar), pH (4, 5, 6), and temperature (30, 40, 50°C) on the permeate flux, total hydraulic resistance, and chemical oxygen demand (COD) rejection of tomato wastewater during nanofiltration treatment was investigated. The flux was found to be approximately constant during long-period operation. The flux was reduced as the pH declined, while it was increased as the temperature and transmembrane pressure increased. The hydraulic resistance (at pH 5 & TMP 1.5 MPa) increased from 5.79×10^{13} to 7.25×10^{13} 1/m when the temperature increased from 30 to 50°C. The COD rejection was ranged from 75.65 to 85.35%, in which the highest value was obtained at pH 6, TMP 2.0 MPa, and 30°C. The response surface methodology results demonstrated that the quadratic, the two-factor interaction (2.Fi), and the linear polynomial models are highly significant for modeling the flux ($R^2 = 0.98$), hydraulic resistance ($R^2 = 0.96$), and COD rejection ($R^2 = 0.90$), respectively. Numerical optimization determined the optimum conditions based on the highest flux and rejection and the lowest fouling with transmembrane pressure of 20 bars, temperature of 30°C, and pH of 6, respectively.

Keywords: Nanofiltration; Modeling; Optimization; Tomato wastewater

1. Introduction

The demand for water consumption is increasing day by day. This fact in addition to increasing scarcity of water resources and social concerns about the impacts of the discharge of wastewater effluent streams on the environment has made situations which incite industries, especially food industry, to reduce water consumption, and to perform efficient effluent treatment for water reuse [1].

Tomato processing industries consume plenty of water; the average amount of wastewater produced in a medium-sized tomato processing factory is about 300 M^3/d. Wastewater from the tomato industry is characterized by a large amount of suspended solids from various stages of processing and consequently high chemical oxygen demand (COD). In the tomato processing industry, wastewater is comprised of water

*Corresponding author.

from tomato washing and trimming (47% total wastewater flow), effluent from scalding and peeling (32% total wastewater flow), canning water (19% total wastewater flow), and concentrator wastewater flows from tomato paste production (2% total wastewater flow) [2]. However, it is important to mention that in this project, wastewater is considered as the material coming directly of cleaning, sorting, and moving tomatoes. This effluent is red, malodorous, and polluted mainly by organics, suspended solids, and ground particles [3]. One of the important issues with this kind of wastewater stream is that it is seasonal (the tomato harvesting lasts 90 d a year) and deteriorates very quickly. Therefore, in this project, samples, which are free of grit material, were transported in batches and stored at −18˚C.

Nanofiltration (NF) is a separation process which is widely utilized for several applications such as water softening, wastewater treatment, chemical, pharmaceutical, food processing industries as well as biotechnologies. NF is defined as pressure-driven membrane processes for the separation and the concentration of substances having a molecular weight between 100 and 1,000 Da [4–6]. NF is one of the promising membrane technologies available for the removal of small molecules without complete desalination [7]. The selectivity factors in NF consist of the function steric effect, electrostatic, dielectric effect due to the fixed charged groups, and solubilization effect due to the swelling capacity [8,9]. According to previous findings in literature, NF leads to a high quality of treated effluent with rejection of salt, color, suspended matter, and COD, respectively, of 47–52, 100, 99.9, and 73–85%, depending on the effluent load [10]. Spiral wound membranes (Desal 5.1 and Desal 5.2 and Filmtec NF4S) have been utilized to decolorize resin-regenerated waste. The NF process allowed 89 and 74% reduction in water and salt consumptions [11]. Multu et al. [12] investigated about decolorization of wastewater of a baker's yeast plant by the membrane process. The obtained results showed maximum rejections of 94, 89, and 72% for OD, color, and COD, respectively. It was noteworthy that 0.8 μm microfiltration membrane and 400 Da NF membrane were used in series. Luo et al. [13] performed two-stage UF and NF processes for the treatment of model dairy wastewater. With this attitude, they demonstrated that most of the dairy wastewater can be recycled to produce reusable water when compared with a single NF process.

Modeling and optimizing are necessary for designing of a new process and better understanding of the present process. Generally, mathematical models that were derived from physical descriptions involve complex equations and need detailed information of the membrane and the process. Therefore, direct analysis with the intelligent systems is an alternative method for description process [14]. One of these methods is response surface methodology (RSM). This method explores the relationships between several independent variables and one or more response variables, which was firstly introduced by Box and Wilson [15]. RSM was successful in modeling and optimizing the membrane processes [16–21]. In addition, there is no study available in the literature exploring the use of RSM for modeling/optimizing the permeate flux, total hydraulic resistance, and COD rejection of NF of the tomato paste wastewater.

The main issue of tomato wastewater treatment lies in the seasonal nature production in the tomato industry. It brings up a need to introduce/develop a technique by which the steady-state condition is reachable quickly and efficiently. It is worth to mention, conventional methods such as active sludge and anaerobic digestion have long period to colt formation, which is not acceptable due to seasonal nature production [2]. This problem makes sense to investigate about a novel technology, such as membrane process, which can reach to the steady-state condition fastly.

Up to now, few investigations have been made on removing pollution from tomato wastewater, using different kinds of membrane technologies. One of the most important investigations was performed by Iaquinta et al. [3]. They optimized NF process of tomato wastewater based on critical flux. It was shown that purification of the wastewater to water compatible with the municipal sewer system requirements is possible, with the recovery rate of 90%. In addition, short-term fouling issues may be avoided at permeate fluxes about or below 8.2 $l\,h^{-1}\,m^2$, but at this project, we optimize NF process of tomato paste wastewater based on the desirability function approach that performs multiple objective optimization. The desirability function acts as a penalty function which leads the algorithm to zone where we can find the desired response variables at the same time.

Therefore, the aims of this paper were: (i) to investigate the performance of polyamide NF membrane for purifying the wastewater from tomato industry, (ii) to study the influence of some operating conditions (pH, temperature, and transmembrane pressure) on permeate flux, total hydraulic resistance, and COD rejection, and (iii) to develop a predictive model using RSM for simulation and optimization of the NF treatment of tomato paste wastewater.

2. Materials and methods

2.1. Equipment

The pilot plant membrane system used in this study has been equipped with a feed tank, reciprocating pump, tubular module, two pressure gages, tubular heat exchanger, two control valves, and temperature sensor (Fig. 1). The membrane was composed of polyamide. The characteristics of NF membrane are summarized in Table 1. The inlet and the outlet feed pressures were monitored by two manual pressure gages. These gages were positioned as close to the inlet and the outlet of the membrane as physically possible. Temperature probe was attached to the feed tank, and employed for monitoring temperature during each run. The temperature of feed was continuously being controlled by a heat exchanger. A permeate collection beaker located on a digital mass balance (±0.05 g) was used to collect permeate, and measured permeate flux (kg/m^2 h) during the experiments. The membrane was rinsed with distilled water before and after each run, and the permeate flux was measured.

2.2. Experimental design

This study investigates the effect of transmembrane pressure at three levels (10, 15, 20 bar), pH at three levels (4, 5, 6), and temperature at three levels (30, 40, 50°C) on the permeate flux, total hydraulic resistance, and COD rejection. A D-optimal design was constructed using of design expert software (version 8/0/7/1, Stat-Ease Corporation, Minneapolis, MN, USA). The D-optimal design maximizes information about the polynomial coefficients. This algorithm selects points that minimize the volume of the confidence ellipsoid for the coefficients. In the other words, it minimizes the determinant of $X{\cdot}X'$ inverse matrix, where X is the matrix of the design, and X' is the transpose of the matrix X [22]. The design was included of a total of 20 experimental runs (Table 2), 10 runs for determining coefficients of model, 5 runs for estimating lack-of-fit, and 5 replications for calculating the error. A quadratic relationship (Eq. (1)) was used to model the responses and the coefficient of determination (R^2) and the adjusted R^2 (R^2_{adj}) were calculated by Eqs. (2) and (3) to assess the efficiency of models and to predict the responses accurately.

$$Y = \beta_0 + \sum_{i=1}^{k} \beta_i X_i + \sum_{i=1}^{k} \beta_{ii} X_i^2 + \sum \sum_{i<j} \beta_{ij} X_i X_j + e \quad (1)$$

$$R^2 = 1 - \frac{SS_{residual}}{SS_{residual} + SS_{model}} \quad (2)$$

$$R^2_{adj} = 1 - \frac{\frac{SS_{residual}}{DF_{residual}}}{\left(\frac{SS_{residual}}{DF_{residual}} + \frac{SS_{model}}{DF_{model}}\right)} \quad (3)$$

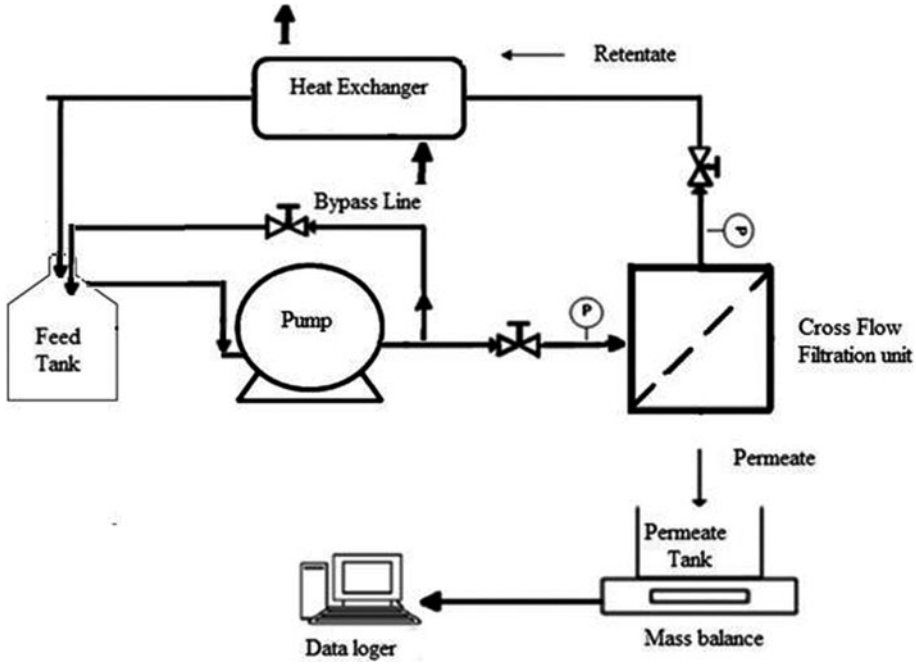

Fig. 1. Schematic diagram of NF pilot plant system used in this study.

Table 1
Characteristics of NF membrane and module used in this study

Membrane type	AFC40 (PCI membranes, Ltd, UK)
Effective area (cm^2)	240
Diameter (mm)	63.5
Length (cm)	30
Range of pH tolerance	1.5–9.5
Maximum temperature (°C)	60
Maximum pressure (MPa)	6
Apparent $CaCl_2$ rejection (%)	60
Module	Tubular (Micro 240, PCI membranes, Ltd, UK)

Table 2
The variables and levels used in D-optimal design for NF treatment of tomato paste wastewater

	Actual value			Variables coded		
	Pressure	pH	Temperature	Pressure	pH	Temperature
1	10	6	50	−1	1	1
2	20	4	50	1	−1	1
3	15	5	40	0	0	0
4	20	5	50	1	0	1
5	20	6	50	1	1	1
6	10	4	30	−1	−1	−1
7	10	5	40	−1	0	0
8	20	5	30	1	0	−1
9	15	5	50	0	0	1
10	15	4	50	0	−1	1
11	20	6	40	1	1	0
12	10	4	50	−1	−1	1
13	15	5	50	0	0	1
14	15	5	40	0	0	0
15	15	5	30	0	0	−1
16	10	5	40	−1	0	0
17	10	6	30	−1	1	0
18	15	6	30	0	1	−1
19	15	4	40	0	−1	0
20	20	5	30	1	0	−1

where Y is the predicted response; X_i is the variables; β_0 is the intercept; β_i is the linear term; β_{ij} is the interaction term, β_{ii} is the quadratic term, e is the residual, DF is the degree of freedom, and SS is the sum of squares. All experimental runs were carried out in duplicate, and the results averaged. The variables were coded based on Eq. (4) in the regression equation:

$$X_j = \frac{U_j - U_j^o}{I_j} \tag{4}$$

where X_j is an independent variable coded value; U_j is an independent variable real value; U_j^o is an independent variable real value in the center point of the independent variable, and I_j is the step change in U_j.

2.3. Measurements

COD method was selected to estimate the organic component concentration in the permeate and feed streams. The COD was measured at 620 nm and 25°C by a MD 200 COD VARIO Photometer (Germany) [23]. The pH was determined by a Lutron YK-2001 pH meter (Taiwan). Dynamic viscosity of permeate samples was measured using an Ostwald U-tube capillary viscometer [24].

2.4. Membrane performance

The rejection of COD was calculated by the following equation:

$$R(\%) = \left(1 - \frac{C_P}{C_F}\right) \times 100 \quad (5)$$

where C_P and C_F are the concentration COD value (mg l^{-1}) in permeate and feed streams, respectively.

The permeate flux (J_P) was calculated by the following relationship:

$$J_P = (W_2 - W_1)/(t \cdot A) \quad (6)$$

The total hydraulic resistance was determined by Eq. (5):

$$R_T = \text{TMP}/(\mu \cdot J_P) \quad (7)$$

where J_P is the permeate flux (m^3/m^2 s), TMP is the transmembrane pressure (Pa), and μ is the viscosity of permeate (Pa s). TMP was measured by the following relationship:

$$\text{TMP} = (P_i + P_o)/2 - P_P \quad (8)$$

where P_i and P_o are inlet and outlet pressures, respectively, and P_P is the permeate pressure.

3. Result and discussions

3.1. Data normality

The normal probability plot shown in Fig. 2 indicates the residuals followed a normal distribution. In the normal distribution, the points will follow a straight line, while in the abnormal distribution; the points have an "S-shaped" pattern, which indicates the necessity for data transformation [25]. It can be seen from Fig. 2 that the points have a normal distribution. In addition, Fig. 3 helps to detect outliers in the data. Points which are beyond the red lines are not fitted well by the current model or are experimental errors [22]. It can be seen from Fig. 3 that all points are in the desired range.

3.2. Permeate flux

The dynamic permeate flux of tomato wastewater NF is shown in Fig. 4. It can be seen that the permeate flux is approximately constant at different TMPs for a long period of time. In addition, at low TMP (10 bar), the permeate flux was reached to steady-state condition in the beginning of NF operation, but with increasing TMP (15 or 20 bar), it need more operation time to reach the steady-state condition. This phenomenon may be explained by studying the effect of increasing TMP on the total hydraulic resistance membrane (Section 3.2). Similar trend was observed for other conditions studied (data not shown). These results suggest the low membrane fouling tendency for this NF membrane surface because of relatively stable flux behavior. The polyamide membranes are inherently hydrophilic and appropriate for tomato wastewater treatment.

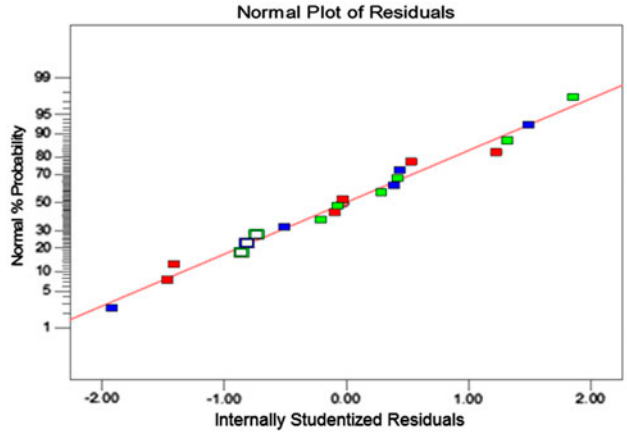

Fig. 2. Normal probability plot vs. internally studentized residuals for permeate flux.

The mean value of the permeate flux was determined by Eq. (9):

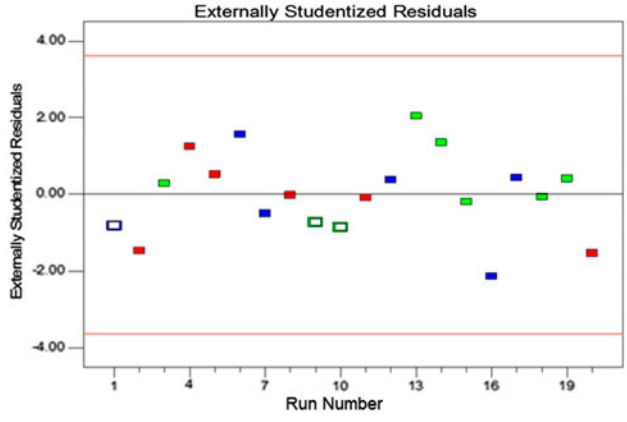

Fig. 3. Externally studentized residual vs. run number for permeate flux.

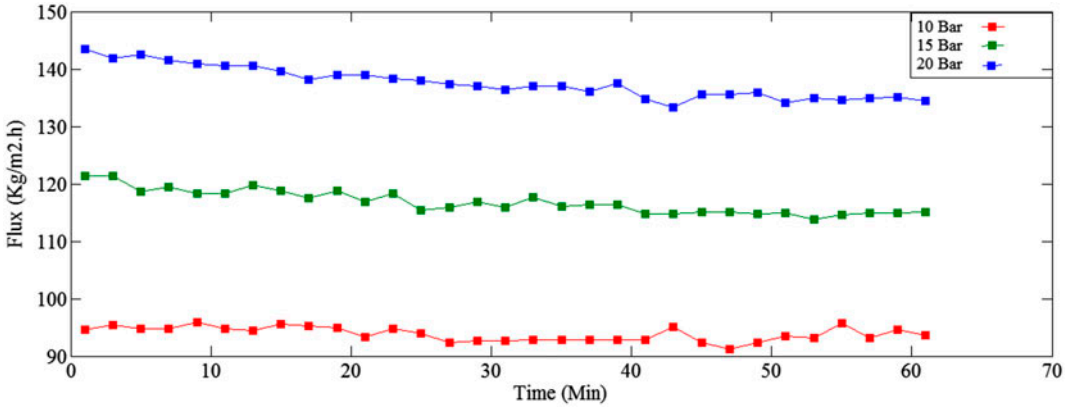

Fig. 4. Dynamic permeate flux during NF process of tomato paste wastewater at various operating TMP (pH 4, Temperature 50℃).

$$J_P = \frac{1}{t_n}\int_0^{t_n} f\,dt \tag{9}$$

where t_n is the overall time of each run (60 min) and f is the permeate flux at time t. The integrals were calculated by the rectangle method by using Matlab2010 (7.10.0).

The results indicated that the quadratic model can acceptably fit the results of the mean permeate flux value (R^2 and R^2_{adj} values equal to 0.98 and 0.96, respectively). The RSM model for prediction of the permeate flux in terms of the coded variables was determined as follows:

$$J_P = 119.66 + 21.58x_1 + 4.32x_2 + 4.38x_3 + 1.62x_1x_2 + 1.07x_1x_3 + 0.27x_2x_3 - 1.45x_1^2 - 3.57x_2^2 + 0.49x_3^2 \tag{10}$$

where x_1 is the transmembrane pressure, x_2 is the pH, and x_3 is the temperature. The least squares regression was utilized to fit the data by Eq. (1). The p-value is used to test the significance of every coefficient. The smaller degree of p, the more significant is the corresponding coefficient. Values of p less than 0.05 show that model terms are significant. It can be seen from

Table 3
Analysis of variance (ANOVA) of factors affecting on the permeate flux

Source	df[a]	MS[b]	F-value	p-Value
Model	9	712.7192	62.48788	<0.0001
A-pressure	1	5,293.387	464.0994	<0.0001
B-pH	1	168.262	14.75242	0.0033
C-temperature	1	218.4546	19.15308	0.0014
AB	1	15.25183	1.337209	0.2744
AC	1	8.077297	0.70818	0.4197
BC	1	0.420496	0.036867	0.8516
A^2	1	9.201184	0.806717	0.3902
B^2	1	48.50425	4.252626	0.0661
C^2	1	1.039513	0.09114	0.7689
Residual	10	11.40572		
Lack-of-fit	5	12.20245	1.1502	0.4409
Pure error	5	10.60898		
Cor total	19			

[a]Degree of freedom.
[b]Mean square.

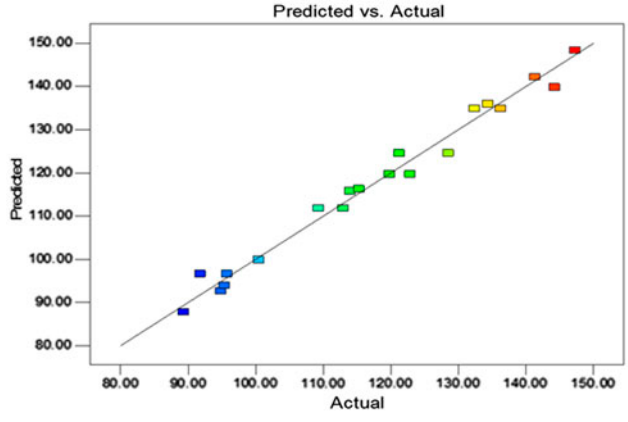

Fig. 5. Correlation between model predictions and experimental permeate flux of NF treatment of tomato paste wastewater (R^2 = 0.98).

Table 3, the linear effects of all parameters and quadratic effect pH were significant ($p < 0.05$). Generally, errors are derived from two sources, lack-of-fit and pure error. Pure error is a measure of the variation in response at same operating condition. It is calculated independently of the regression. The lack-of-fit is calculated as the difference between total error and pure error. It can be seen from Table 3, the lack-of-fit test is not significant, suggests that the quadratic model is desirable for prediction permeate flux.

The coefficient of determination was 0.98, which represents the fact that the statistical model can explain 98% of the variability in the response. A high value of the adjusted determination coefficient (0.96) also supports a high significance of the corresponding model shown in Fig. 5. The high ability of model to predict permeate flux can decrease the cost of experiments and save time.

The effect of TMP and pH as well as TMP and temperature on the permeate flux is shown in Figs. 6 and 7, respectively. It can be seen that the permeate flux was increased by increasing the pH value. This is due to the fact that the pH of feed can change the ionization of particular functional group on the membrane surface, e.g. carboxyl and amine. As a result, these functional groups repel each other because of the electrostatic force. Accordingly, the pore becomes wider and the volume value increases. It can be found that the permeate flux was increased by 6.07% with one unit increase in pH.

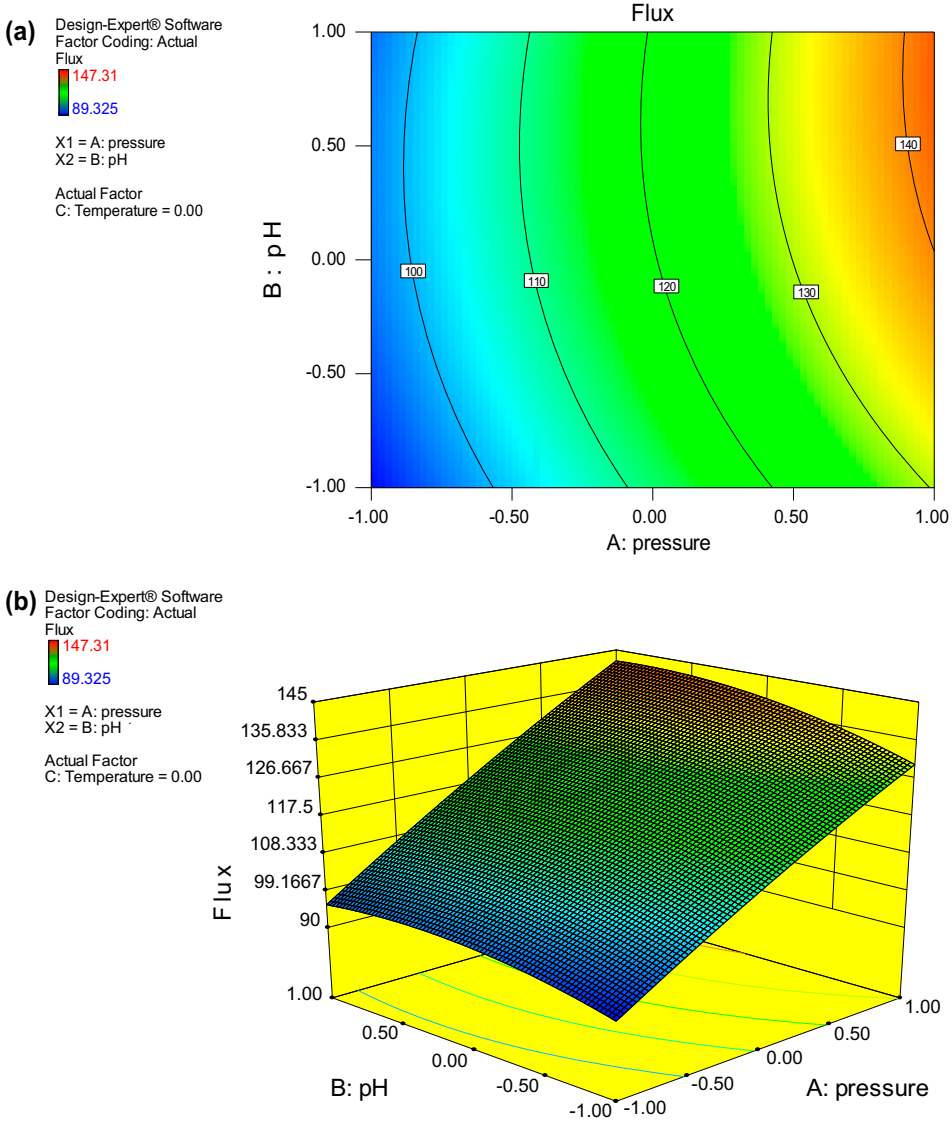

Fig. 6. The combined effects of pH and pressure on the permeate flux (40°C); (a) Contour plot and (b) Response plot.

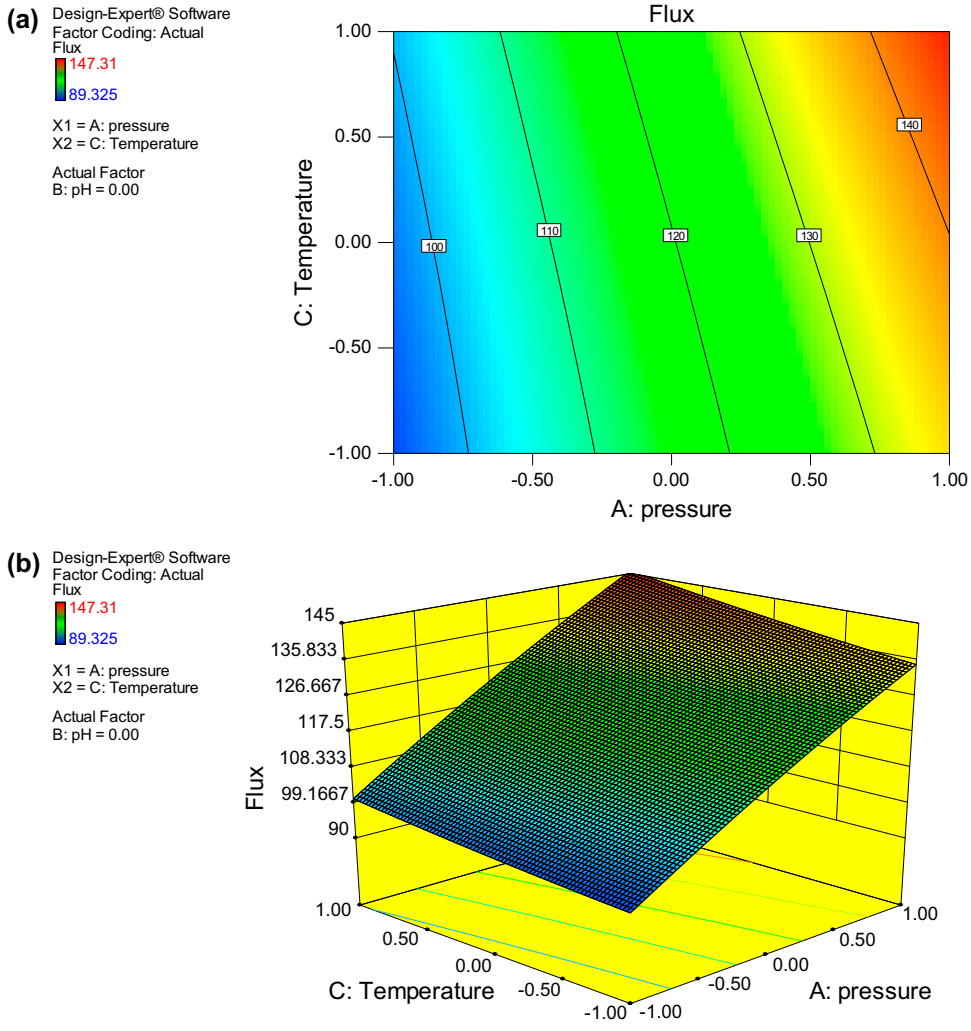

Fig. 7. The combined effects of temperature and pressure on the permeate flux (pH 5); (a) Contour plot and (b) Response plot.

Transmembrane pressure enhanced the permeate flux because of the increase in the driving force. In this research, the permeate flux was found to be pressure-dependent zone. According to Table 4, the permeate flux was increased about 4.85% when TMP increased 1 bar. The maximum permeate flux (147.31 kg/m^2 h) was obtained at pressure 20 bar, pH 6, and temperature 50˚C. As shown in Fig. 7, the average permeate flux (at pH 5 and TMP 1.5 MPa) was linearly increased from 114 to 128.5 kg/m^2 h with increase in temperature from 30 to 50˚C. In other words, the permeate flux was increased almost 0.5% with one degree Celsius increase in temperature (Table 4). This is due to the fact that the fluid viscosity

Table 4
Effect of increasing temperature, pH, and transmembrane pressure (TMP) on change percentage of permeate flux, hydraulic resistance, and COD rejection in the NF treatment of tomato paste wastewater

Process variable	Flux	Hydraulic resistance	COD rejection
Temperature (˚C)	+0.50	+1.70	−0.21
pH	+6.07	−3.50	+0.92
Pressure (bar)	+4.85	+2.00	+0.38

and the concentration polarization decrease, whereas the diffusivity coefficient increases. Therefore, it can be concluded that solutes and water can easily pass through the membrane. These results are consistent with the earlier observation [4,26–29].

3.3. Total hydraulic resistance

The results indicated two-factor interaction model (2.Fi) is highly significant for prediction of the total hydraulic resistance in the NF treatment of tomato paste effluent. The RSM model for the R_T in terms of the coded variables was obtained as follows:

$$R_T = (6.7 + 1.15x_1 - 0.279x_2 - 0.905x_3 - 0.113x_1x_2 - 0.18x_1x_3 - 0.0038x_2x_3) \cdot 10^{13} \quad (11)$$

The R^2 and R^2_{adj} values for above equation were 0.96 and 0.94, respectively. Insignificant the lack-of-fit test and F-value (53.65) indicate that the model is sufficiently accurate for predicting the total hydraulic resistance (R_T). Furthermore, the coefficient of variation value (4.25%) indicates the acceptable reproducibility. According to Table 5, the linear effect of all parameters and interaction effect pressure and temperature were significant ($p < 0.05$). In addition, an excellent agreement between prediction and experiment results (R^2=0.96) was achieved (Fig. 8). These results indicated the desirability of D-optimal design for statistical assessment of tomato wastewater treatment with minimal testing.

The effect of TMP and temperature on R_T is shown in Fig. 9(a) and (b). It can be seen that R_T is augmented because of increase in the transmembrane pressure and temperature. The effect of the pressure on R_T is due to the fact that increase in the pressure augments the rate of migrating compounds toward the membrane surface and pores. As a result, the precipitation of these compounds on the membrane increases by the convective transport [14]. According to Table 4, the R_T value increased almost 2% when the transmembrane pressure increased by 1 bar. On the other hand, R_T decreased about 3.5% with one unit increase in pH. This phenomenon may be due to the effect of pH on the ionization of carboxyl groups of pectin in feed. Increasing pH probably prevented joining of the pectin molecules; as a result, total hydraulic resistance was decreased.

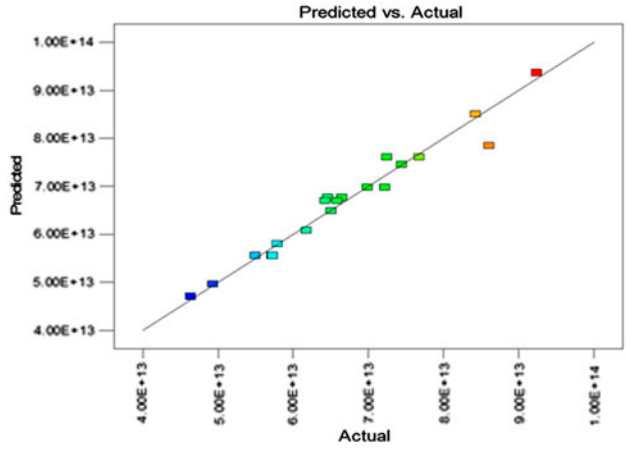

Fig. 8. Correlation between model predictions and experimental total hydraulic resistance of NF treatment of tomato paste wastewater (R^2 = 0.96).

Table 5
Analysis of variance (ANOVA) of factors affecting on the total membrane hydraulic resistance

Source	df	MS	F-value	p-Value
Model	6	4.37E+26	53.6501	<0.0001
A-pressure	1	1.53E+27	188.2244	<0.0001
B-pH	1	7.25E+25	8.903044	0.0106
C-temperature	1	9.57E+26	117.5524	<0.0001
AB	1	7.73E+24	0.949182	0.3477
AC	1	2.59E+25	3.183213	0.0977
BC	1	8.78E+23	0.107812	0.7479
Residual	13	8.14E+24		
Lack-of-fit	8	1.1E+25	3.129799	0.1122
Pure error	5	3.52E+24		
Cor total	19			

The temperature showed a significant effect on R_T. When the temperature increases, the concentration polarization will decrease, whereas turbulent flow will increase. These factors decrease the total hydraulic resistance. On the contrary, the R_T value increased due to increase in the temperature. This is because the fact that molecules in the low temperature have low energy activation, so that these molecules are adsorbed on the membrane with the weak bonding such as the hydrogen bounding. However, at the high temperature, chemical reactions influence the interaction between solutes and membrane. Therefore, it can be concluded that increasing temperature can increase the R_T [30]. Furthermore, R_T (at pH 5 and TMP 1.5 MPa) was increased from 5.79×10^{13} to 7.25×10^{13} 1/m with increase in temperature from 30 to 50˚C, In other words, the total hydraulic resistance was increased almost 1.7% with 1˚C increase in temperature (Table 4).

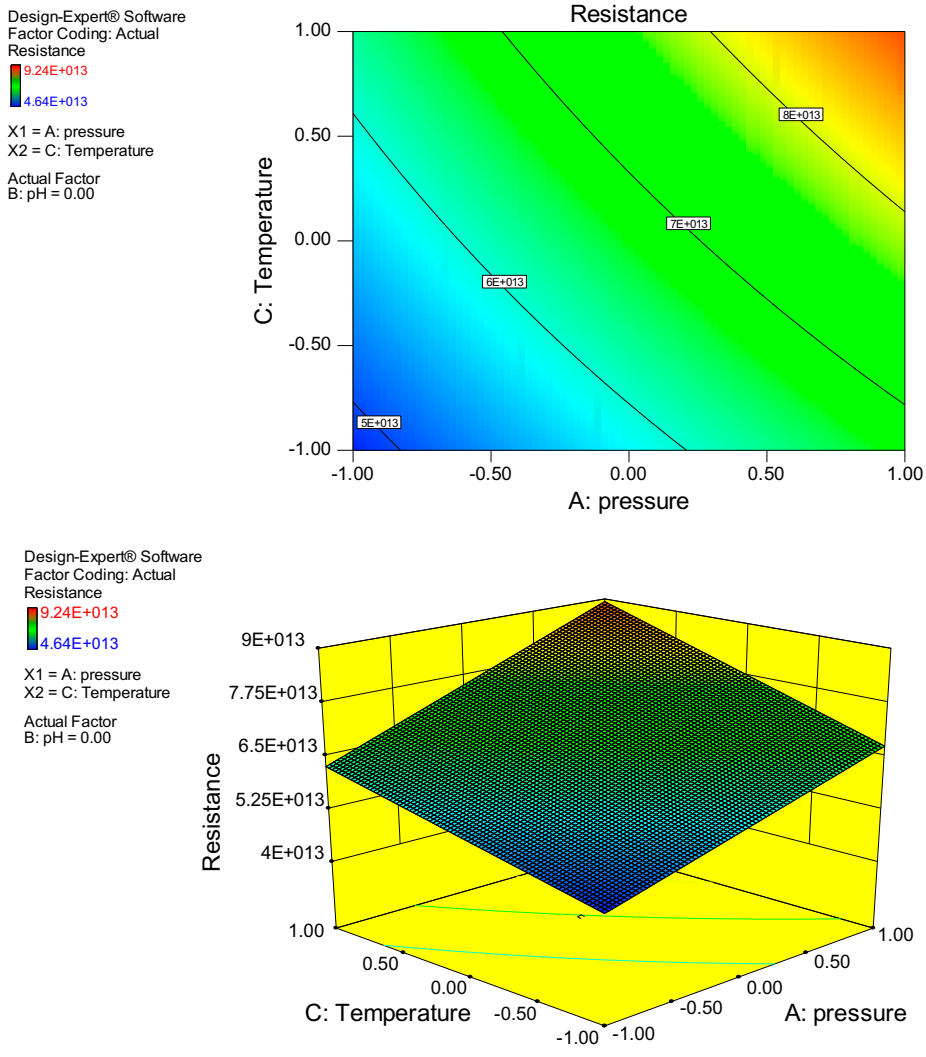

Fig. 9. The combined effects of temperature and pressure on the overall resistance (pH 5); (a) Contour plot and (b) Response plot.

Table 6
Analysis of variance (ANOVA) of factors affecting on the COD rejection

Source	df	MS	*F*-value	*p*-Value
Model	3	64.7819	50.7231	<0.0001
A-pressure	1	178.6454	139.8763	<0.0001
C-pH	1	3.115078	2.439054	0.1379
B-temperature	1	5.820093	4.557035	0.0486
Residual	16	1.277167		
Lack-of-fit	11	1.483929	1.804632	0.2671
Pure error	5	0.822289		
Cor total	19			

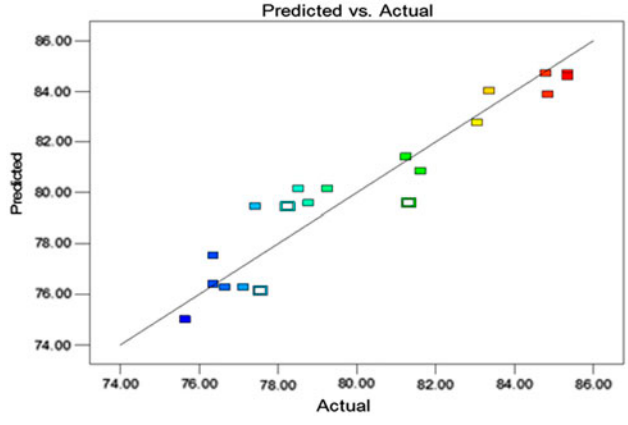

Fig. 10. Correlation between model predictions and experimental COD rejection of NF treatment of tomato paste wastewater (R^2 = 0.90).

3.4. COD rejection

The linear relation was obtained with high significance and good predictive value. The R^2 and adj-R^2 values (0.90 and 0.88, respectively) prove the model adequacy for describing the relation between the independent variables and the COD rejection. The RSM model for prediction of the COD rejection in terms of the coded variables was determined as follows:

$$R_{COD} = 80.146 + 3.875x_1 + 0.563x_2 - 0.7x_3 \quad (12)$$

The ANOVA approach is applied to investigate which factors significantly affect the response parameters. According to Table 6, statistical analysis displayed that in the linear model of the COD rejection, the linear effects of all parameters except pH are significant ($p < 0.05$). "Adeq Precision" measures the signal to noise ratio. This parameter compares the range of the predicted values at the designed points to the average prediction errors [25]. In this study, a ratio greater than 4 is desirable. The ratio of 19.21 for COD removal indicates an adequate signal. The determination coefficient value for estimation of COD rejection was 0.90, which indicates high correlation between predicted and experimental values (Fig. 10). The ability to predict J_P, R_T, and COD rejection could reduce the computation time and the amount of practical

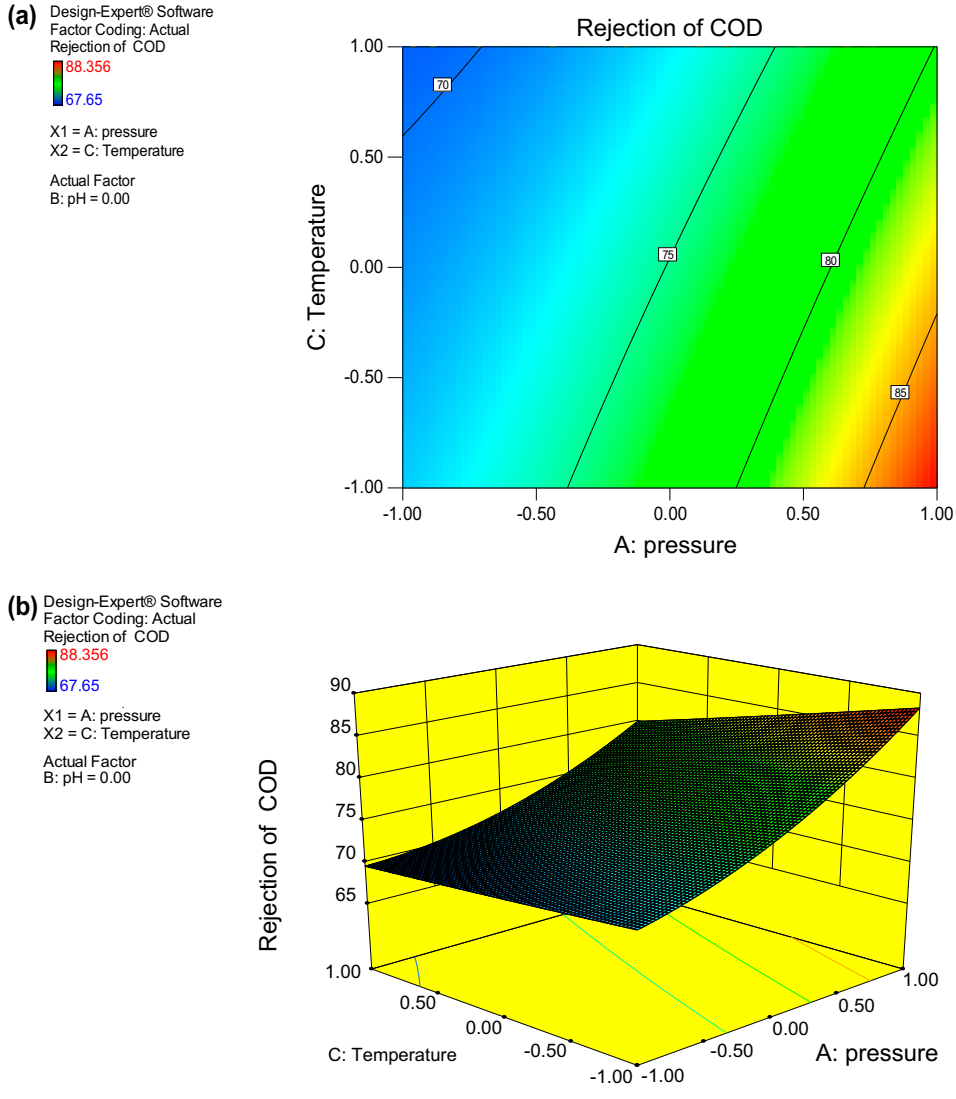

Fig. 11. The combined effects of pressure and temperature on the COD rejection (40°C); (a) Contour plot and (b) Response plot.

Table 7
Optimization of NF treatment of tomato paste wastewater

Process variable	Optimum value	Actual value	Goal	Lower limit	Upper limit	Desirability
Pressure (bar)	20	20	In range	10	20	0.86
Temperature (℃)	30	30	In range	30	50	
pH	6	6	In range	4	6	
Flux (kg/h m^2)	137	129.8	Max	89.325	147.31	
R_T (1/m) × 10^{13}	6.41	6.78	Min	4.64	9.24	
COD rejection (%)	85.28	80.2	Max	75.65	85.356	

work required before designing a new membrane process.

Fig. 11(a) and (b) shows the surface plot and contour plot of the interactive effect of TMP-temperature on COD rejection. It can be seen that with increasing the TMP and decreasing the temperature, the COD rejection increased, and maximum rejection was obtained at maximum TMP and minimum temperature. The effect of pressure can be explained that permeate flux increases with the pressure more than the solute flux (dilute effect). Also, effect of compaction membrane can increase COD rejection and should not be neglected. In addition, according to Table 4, It can be found that the COD rejection increased by almost 0.38 and 0.92% as the TMP and pH increased 1 bar and one unit, respectively.

Increasing temperature causes an increase in solutes diffusion coefficient. Furthermore, such increase in temperature can cause membrane relaxation (increasing membrane effective pore radius). As a result, strict exclusion effect can be decreased and solutes can pass through the membrane easily. The rejection of COD decreased from 81.6 to 77.4% with increasing the temperature from 30 to 50℃. Furthermore, it can be found that the COD rejection decreased approximately 0.21% with the unit change in temperature (at constant conditions of pH 5 and TMP 1.5 MPa) (Table 4). These results are consistent with those reported earlier [4,28,29,31,32].

3.5. Optimization process

In this paper, the desirability function approach was used to perform multiple optimizations. This approach starts firstly by converting each response variable into a desirability function *di*, which varies from 0 to 1, where if the response *yi* is at its target, then $di = 1$, and if the response is outside of an acceptable region, $di = 0$. Global desirability function is determined by Eq. (13). This method should search for response variable values where *D* tends to 1.

$$D = (d_1 \cdot d_2 \cdot d_3 \ldots d_m)^{1/m} \tag{13}$$

Numerical optimization determined the optimum conditions based on the highest permeate flux and rejection and the lowest total hydraulic resistance. The final result of this optimization suggested that the transmembrane pressure of 20 bar, temperature of 30℃, and pH of 6 were the optimum conditions under which the best performance of treatment process by NF was achieved. The desirability function had been achieved to be 0.86 which indicates the high accuracy of optimization. There was no significant difference between experimental and predicted values at optimum condition (Table 7).

4. Conclusion

The NF process was presented for tomato wastewater treatment. The permeate flux, COD rejection, and hydraulic resistance were affected by TMP, temperature, and pH. Referred to numerical optimization, the best performance for the treatment by NF was achieved under the conditions with transmembrane pressure of 20 bars, temperature of 30 C, pH of 6. At most of the experimental runs, no serious case of fouling was observed. From the environmental standpoint, it seems that under a known operating condition, NF can be utilized as an efficient process for the wastewater treatment of tomato processing plant. Based on the results attained in this research, it is not required to increase pH and temperature of feed to obtain the optimal operating condition, which is very important from an industrial point of view.

References

[1] S. Madaieni, M. Ghanei, Reuse as a solution for water shortage in Iran, in: The 2nd International Conference on Water Resources and Arid Environment, Riyadh, Saudi Arabia, 2006.

[2] R.M.A Napoli, A study on treatment of wastewater from a peeled-tomato factory, Agric. Waste 1 (1979) 143–156.
[3] M. Iaquinta, M. Stoller, C. Merli, Optimization of a nanofiltration membrane process for tomato industry wastewater effluent treatment, Desalination 245 (2009) 314–320.
[4] F. Salehi, S.M.A. Razavi, M. Elahi, Purifying anion exchange resin regeneration effluent using polyamide nanofiltration membrane, Desalination 278 (2011) 31–35.
[5] L.A. Coral, L.A.D.O. Proença, F.D.J. Bassetti, F.R. Lapolli, Nanofiltration membranes applied to the removal of saxitoxin and congeners, Desalin. Water Treat. 27 (2011) 8–17.
[6] S.A. Avlonitis, D.A. Avlonitis, S. Skourtis, D. Vlachos, An experimental and modeling study of nanofiltration processes for mixed electrolyte solutions, Desalin. Water Treat. 7 (2009) 25–34.
[7] A. Wahab Mohamad, A modified Donnan-steric-pore model for predicting flux and rejection of dye/NaCl mixture in nanofiltration membranes, Sep. Sci. Technol. 37 (2002) 1009–1029.
[8] M. Taleb-Ahmed, S. Taha, R. Maachi, G. Dorange, The influence of physico-chemistry on the retention of chromium ions during nanofiltration, Desalination 145 (2002) 103–108.
[9] M.J. López-Muñoz, A. Sotto, J.M. Arsuaga, Nanofiltration removal of pharmaceutically active compounds, Desalin. Water Treat. 42 (2012) 138–143.
[10] N. Tahri, G. Masmoudi, E. Ellouze, A. Jrad, P. Drogui, R. Ben Amar, Coupling microfiltration and nanofiltration processes for the treatment at source of dyeing-containing effluent, J. Clean. Prod. 33 (2012) 226–235.
[11] S. Cartier, M.A. Theoleyre, M. Decloux, Treatment of sugar decolorizing resin regeneration waste using nanofiltration, Desalination 113 (1997) 7–17.
[12] S.H. Mutlu, U. Yetis, T. Gurkan, L. Yilmaz, Decolorization of wastewater of a baker's yeast plant by membrane processes, Water Res. 36 (2002) 609–616.
[13] J. Luo, L. Ding, B. Qi, M.Y. Jaffrin, Y. Wan, A two-stage ultrafiltration and nanofiltration process for recycling dairy wastewater, Bioresour. Technol. 102 (2011) 7437–7442.
[14] S.M.A. Razavi, A. Mortazavi, S.M. Mousavi, Dynamic modelling of milk ultrafiltration by artificial neural network, J. Membr. Sci. 220 (2003) 47–58.
[15] G.E.P. Box, K.B. Wilson, On the experimental attainment of optimum conditions, J. R. Stat. Soc. Series B. 13(1) (1951) 1–45.
[16] A.L. Ahmad, C.P. Leo, S.R.A. Shukor, Statistical design of experiments for dye–salt–water separation study using bimodal porous silica/γ-alumina membrane, Desalin. Water Treat. 5 (2009) 80–90.
[17] J.M. Gohil, A.K. Suresh, Development of high flux thin-film composite membrane for water desalination: a statistical study using response surface methodology, Desalin. Water Treat. 52 (2013) 5219–5228.
[18] Y.J. Kim, J. Jung, S. Lee, J. Sohn, Modeling fouling of hollow fiber membrane using response surface methodology, Desalin. Water Treat. 54 (2015) 966–972.
[19] T. Mohammadi, P. Kazemi, M. Peydayesh, Optimization of vacuum membrane distillation parameters for water desalination using Box–Behnken design, Desalin. Water Treat. (in press) 1–10.
[20] A. Hedayati Moghaddam, J. Shayegan, J. Sargolzaei, T. Bahadori, Response surface methodology for modeling and optimizing the treatment of synthetic starchy wastewater using hydrophilic PES membrane, Desalin. Water Treat. 51 (2013) 7036–7047.
[21] M. Sadeghian, M. Sadeghi, M. Hesampour, A. Moheb, Application of response surface methodology (RSM) to optimize operating conditions during ultrafiltration of oil-in-water emulsion, Desalin. Water Treat. (in press) 1–9.
[22] Design expert, Design Expert Software User's Guide, (Version 8/7/0/1). Design expert, Inc., Minneapolis, 2010.
[23] R.L. Droste, Theory and Practice of Water and Wastewater Treatment, Wiley, New York, NY, 1997, pp. 94–132.
[24] J.F. Steffe, Rheological Methods in Food Engineering, Freeman press, East Lansing, 1996, pp. 94–156.
[25] J. Sargolzaei, A. Hedayati Moghaddam, J. Shayegan, Statistical assessment of starch removal from starchy wastewater using membrane technology, Korean J. Chem. Eng. 28 (2011) 1889–1896.
[26] A. Abbas, N. Al-Bastaki, Modeling of an RO water desalination unit using neural networks, Chem. Eng. J. 114 (2005) 139–143.
[27] A. Salahi, I. Noshadi, R. Badrnezhad, B. Kanjilal, T. Mohammadi, Nano-porous membrane process for oily wastewater treatment: Optimization using response surface methodology, J. Environ. Chem. Eng. 1 (2013) 218–225.
[28] F. Salehi, S.M.A. Razavi, Dynamic modeling of flux and total hydraulic resistance in nanofiltration treatment of regeneration waste brine using artificial neural networks, Desalin. Water Treat. 41 (2012) 95–104.
[29] Y. Babaee, S.M. Mousavi, S. Danesh, A. Baratian, Influence of transmembrane pressure and feed concentration on the retention of aresnic, chromium and cadmium from water by nanofiltration, Environ. Sci. Eng. 52 (2010) 1–6.
[30] K.F. Eckner, E.A. Zottola, Partitioning of skim milk components as a function of pH, acidulant, and temperature during membrane processing, J. Dairy Sci. 75 (1992) 2092–2097.
[31] J. Wang, Y. Wei, Y. Cheng, Advanced treatment of antibiotic wastewater by nanofiltration: Membrane selection and operation optimization, Desalin. Water Treat. 52 (2013) 7575–7585.
[32] M. Nilsson, F. Lipnizki, G. Trägårdh, K. Östergren, Performance, energy and cost evaluation of a nanofiltration plant operated at elevated temperatures, Sep. Purif. Technol. 60 (2008) 36–45.